Magnetically Controlled Multifunctional Capsule Robot for Dual-Drug Delivery

Lingling Zheng, *Student Member, IEEE*, Shuxiang Guo, *Fellow, IEEE*, and Masahiko Kawanishi

***Abstract*—This article presents a multifunctional capsule robot (MCR) with active locomotion, dual-drug load, and selective drug release. The MCR has a high ratio of the volume of loaded drug to the total volume of the capsule (RDC) and can provide sufficient dosages for treatment. The MCR might be used to address the limitations in robot-assisted drug delivery, greatly improving the efficiency of intestinal disease treatment. The MCR is composed of a locomotion unit and a drug delivery unit, and these units are controlled by two orthogonal rotating magnetic fields. This proposed MCR enables active locomotion to target positions and selects to release two different drugs according to clinic requirements. *In vitro* and *ex vivo* experiments were conducted to evaluate the performance of the MCR. Experimental results show that the maximum drug loading capacity of the MCR is 1.5 g, and the maximum advance and retreat velocities are 11.8 mm/s and 10.4 mm/s, respectively, when the MCR is fully loaded. The MCR can release two different drugs in various targets and no noticeable damages to the pig intestine were observed to the naked eyes. The MCR will have potential further application for intestinal disease treatment.**

***Index Terms*—Active locomotion, dual-drug delivery, intestinal disease treatment, magnetically controlled robot, multifunctional capsule robot (MCR).**

I. Introduction

GASTROINTESTINAL (GI) endoscopy usually uses a flexible tube with a camera inserted from the mouth or anus to the nidus for diagnosis and treatment. It mainly consists of the upper GI endoscopy and lower GI endoscopy. The upper GI endoscopy can detect the esophagus, stomach, and the first part of the small intestine (duodenum); the lower GI endoscopy examines the colon and rectum [1]. Most intestine areas have difficulty being tested due to the long distance from the mouth and anus. The GI endoscopy also brings discomfort to patients during procedures. So, wireless capsule robots have become a promising tool for diagnosis and treatment in the intestine that would be the most inaccessible part of the GI tract [2], [3].

Common commercial capsule robots passively move in the intestinal tract by peristalsis and contractions of the intestine. Since this passive movement method lacks precise control over the position and speed of capsule robots, the operating time and the missed diagnosis rate will increase [4], [5]. Therefore, it is significant to develop active capsule robots that can be manipulated remotely in the intestinal tract. Many active capsule robots are capable of being equipped with the diagnosis mechanisms allowing the gastroenterologist to diagnose patients' intestinal conditions using captured images. However, patients suspected of having intestinal diseases may need further treatment and these capsule robots have limited applications due to the lack of further treatment functions. Therefore, capsule robots with drug delivery have been investigated due to the effective treatment in the GI tract.

Nam *et al.* [6] developed a microrobot composed of two rotating cylindrical magnets, four fixed cylindrical magnets, and a helical body. Two orthogonal rotating magnetic fields along the moving direction were used to generate axial locomotion. This microrobot employed an external rotating magnetic field to rotate the cylindrical magnets eccentrically and then the drug in the slot of the front cylindrical magnets was squeezed and discharged through the front nozzle. Kim and Ishiyama [7] proposed a magnetic robot with a targeted drug release mechanism based on active locomotion. This robot is manipulated by a three-axis Helmholtz coil system and can conduct drug release by two spiral components. In [8], a drug-delivery capsule was proposed to achieve accurate drug release in the GI tract. The capsule uses a one-way valve, two axially magnetized cylindrical magnets, and a multilayer solenoid coil to control the drug delivery. When the multilayer solenoid coil is activated, the drug champer will be squeezed so that the drug flows out of the valve. During the procedures with capsule robots, patients need to swallow capsules, and apparently, the capsule with smaller dimensions will be easier to be orally taken, which is better for patient compliance. Capsules can be considered swallowable when they are similar to 11 mm in diameter and 26 mm in length [9]. Nevertheless, released drugs need to be guaranteed to have a sufficient dosage for treatment, which brings a requirement on the volume of drugs loaded by capsules. Hence, the capsule robots are required to have a high ratio of the volume of loaded drug to the total volume of the capsule (RDC) [10]. Most currently developed robots possess lower RDCs, such as the RDCs of 0.16 and 0.28 in [7] and [8], respectively, while it will be better to have an RDC of more than 0.4 for further application [10]. Beccani *et al.* [11] developed a magnetic drug delivery capsule driven by a coil actuation mechanism. The drug release is performed by separating the drug release cage and

Manuscript received July 9, 2021; revised November 30, 2021; accepted January 20, 2022. *(Corresponding author: Shuxiang Guo.)*

Lingling Zheng is with the Graduate School of Engineering, Kagawa University, Takamatsu 761-0396, Japan (e-mail: zhenglingling2018@outlook.com).

Shuxiang Guo is with the Faculty of Engineering and Design, Kagawa University, Takamatsu 761-0396, Japan, and also with the Key Laboratory of Convergence Medical Engineering System and Healthcare Technology, Ministry of Industry and Information Technology, Beijing Institute of Technology, Beijing 100081, China (e-mail: guo.shuxiang@kagawa-u.ac.jp).

Masahiko Kawanishi is with the Faculty of Medicine, Kagawa University, Takamatsu 761-0793, Japan (e-mail: mk@kms.ac.jp).

Digital Object Identifier 10.1109/JSYST.2022.3145869

drug chamber with the magnetic field. Since the mechanism has a small size, the RDC increases to 0.6. This high RDC will allow the capsule to load more drugs, and however, same to current capsule robots, this capsule can only release one type of drug while more drugs would be needed during the treatment [10]. For example, some drugs are only effective when mixed, or different lesions need various drugs. In the past few years, we developed various magnetically controlled capsule robots that can move actively in the pipe and achieve drug delivery [12]–[16]. These capsule robots were equipped with a spiral structure or a jet motion mechanism to achieve free movement in the tube environment. Various methods were employed to release drugs, but these capsule robots still had low RDCs and failed to load and release multiple drugs. In summary, the high RDC and multidrug delivery are two issues for the capsule robots in the article.

In this article, to overcome the limitations mentioned above, we propose a multifunctional capsule robot (MCR) with high DRC and selective dual-drug delivery. It can load two different drugs, move to target positions, and release selected drugs according to clinic requirements. The main contributions of this article are as follows.

1) A dual-drug delivery concept was proposed and integrated with the active capsule robot. This concept enables one single capsule robot to perform more complex treatments and eliminates multiple robots to release various drugs.
2) A dual-drug release mechanism was developed to perform selective drug release. The drug release mechanism uses two limit positions to set the release magnet's rotation angles instead of precise control. Besides, this method also creates more spatial potential for drug loading and allows capsule robots to have higher RDCs that can provide sufficient dosage for treatment. With the dual-drug delivery and high RDC, the treatment cost could be reduced and the treatment efficiency would be improved.
3) A control method was developed to control the dual-drug release mechanism. This control method employs a constant magnetic field and rotating magnetic field to determine the MCR pose and select various drugs for release. This method achieves stable control of dual-drug release with the open-loop control and without changing the existing equipment and adding additional components, thus reducing the control difficulty and improving the control reliability and adaptability to complex environments.

This article is organized as follows. Section II presents the clinical requirement, robot design, motion analysis, dual-drug release control, prototype, and clinic considerations of the proposed MCR. Experiments evaluating the performance of the proposed MCR, including locomotion, drug release control, dual-drug release test, and *ex vivo* experiments, are detailed in Section III. Conclusion and future work are summarized in Section IV.

II. Design of the Multifunctional Capsule Robot

A. Clinical Requirements

During the process of treatment, various drugs are selected and released according to different treatment requirements. It would be inadequate for capsule robots to load and release one kind of drug. For example, hemostatic and anti-inflammatory drugs are commonly needed to treat intestinal diseases and would be regularly employed at the same time. Existing capsule robots generally are able to carry and release one kind of drug, such as the robots in [8] and [11]. Therefore, multiple capsule robots will be needed and swallowed multiple times by patients when this type of capsule robot is used for treatment. In order to enable one single capsule robot to load multiple drugs and then achieve selective drug release at various target positions, multiple drug storehouses are required to be integrated into one single capsule robot. Besides, a control mechanism for drug storehouses needs to be developed to control the opening and closing of the drug storehouse, so as to maintain the selective drug release.

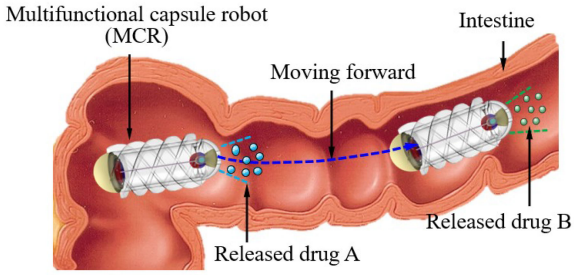

Fig. 1. Concept of the MCR.

To provide capsule robots with active movement discussed in Section I, power issues need to be considered [17]. Active capsule robots can be classified as battery-powered and battery-free ones, depending on the presence and absence of batteries set inside the robot bodies. Battery-powered capsule robots are equipped with motors and batteries and are able to move with the rotation driven by the motors; battery-free capsule robots achieve locomotion through the external driving magnetic field and the magnet set inside the robot. Using the magnetic field avoids harmful battery substances entering the body [17]. The absence of batteries and internal locomotion systems allows the capsule robot to have spatial potential that can be used for other diagnostic and therapeutic considerations [18]. Therefore, this battery-free mode will be chosen in this article due to the higher safety and more space it possesses [17], [18]. Moreover, in this article, the number of drug storehouses is set as two, and the control principle of the two storehouses will be explored. Therefore, the design requirements for the capsule robot include advance and retreat of the capsule robot and independent control of dual-drug release. As shown in Fig. 1, the desired capsule robot carrying two drugs moves in the intestine and releases drugs at target positions: moving to the location where treatment is needed and releasing drug A; continuing to move to another target position and releasing drug B.

B. Robot Design

When multiple magnets are applied in a magnetic field, they will interfere with each other, so the number of magnets embedded in the capsule robot will be limited. Reducing the number

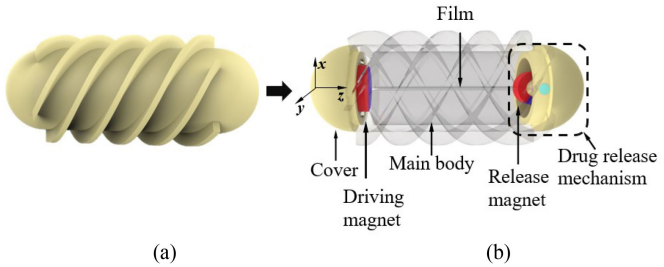

Fig. 2. Structure of the MCR. (a) Front view. (b) Internal structure.

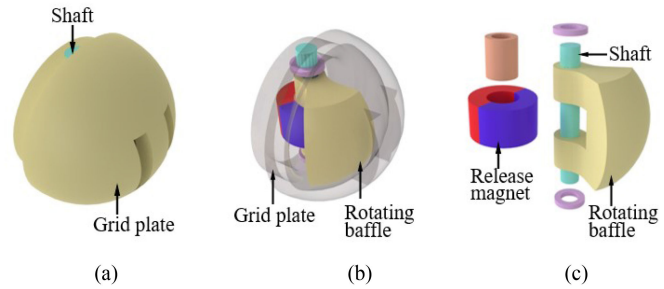

Fig. 3. Structure of the drug release mechanism. (a) Front view. (b) Internal structure. (c) Exploded view.

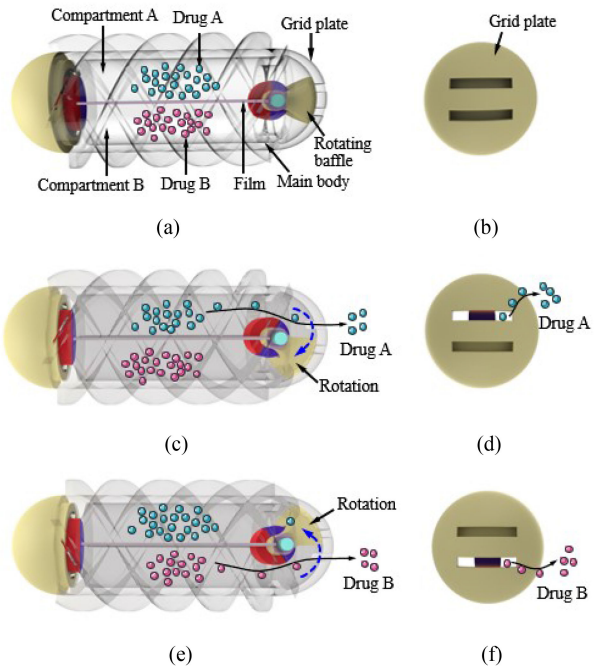

Fig. 4. Diagram of drug release process. (a) Capsule robot loading drugs A and B, and the rotating baffle located at the median position of the grid plate. (b) Side view of (a). (c) Drug A released from compartment A. (d) Side view of (c). (e) Drug B released from compartment B. (f) Side view of (e).

of magnets will facilitate the stable control of the capsule robot. For this reason, the number of magnets in this article is set as two: one for the advance and retreat of the capsule robot and the other one for independent control of dual-drug release. Besides, it will be difficult to achieve precise rotation control of the magnet inside the capsule robot due to the complex intestine environment. Therefore, it is necessary to develop a suitable mechanism that can complete independent control of dual-drug release only using a single magnet.

In this article, two magnets are used and set at the ends of the capsule robot and their axes are perpendicular to each other. One magnet, named as driving magnet, can drive the robot to move and its axis is coaxial with the z-axis. The other one, i.e., release magnet, used to manipulate the drug release mechanism achieving the release of different drugs, is coaxial with the y-axis (see Fig. 2). The driving magnet is installed at the end of the main body and can rotate the capsule robot when the external rotating magnetic field is applied. The outer side of the main body is equipped with spiral wings, which can generate propelling force to the capsule robot when the capsule robot rotates. By controlling the direction of the magnetic field, the forward and reverse rotation of the capsule robot can be realized so that the capsule robot will move forward and backward. As shown in Fig. 3, the drug release mechanism comprises a shaft, rotating baffle, release magnet, and grid plate. The release magnet is installed on the shaft that is assembled in the hole set by the rotating baffle. The rotating baffle has a spherical end and can form a sealed fit with the grid plate. The release magnet drives the rotating baffle to rotate and thus the relative position of the hole on the grid plate can be adjusted according to the requirements.

As shown in Fig. 4, the main body of the MCR is divided into compartment A and compartment B through a film. Compartments A and B are used to hold different drugs, i.e., drugs A and B. The drug release mechanism is installed at the end of MCR to realize the selective drug release. There are two grid holes on the grid plate, and the initial position of the rotating baffle is in the middle of the grid plate [see Fig. 4(a)]. At this position, both grid holes are blocked by the rotating baffle and are in a closed state. Drugs A and B will be stored in compartments A and B without being released. When drug A needs to be released, the release magnet will be rotated by an external magnetic field [see Fig. 4(c)]. The release magnet keeps driving the rotating baffle to rotate until the rotating baffle reaches the limit position. At this time, the rotating baffle stops moving, even if the external magnetic field is still trying to drive the release magnet to rotate. As shown in Fig. 4(c) and (d), compartment A joins the external environment, and drug A enters the intestine through the hole on the grid plate. Similarly, as shown in Fig. 4(e) and (f), the magnetic field rotates the release magnet in the opposite direction. The rotating baffle moves to the other limit position and compartment B joins the external environment. Drug B in compartment B then enters the intestine through the other holes on the grid plate.

C. Motion Analysis

When the MCR needs to move forward or backward, the driving magnet rotates with the rotation of the rotating magnetic field. During these processes, the driving magnet is driven by the rotating magnetic field but is also affected by the release magnet even if the release magnet is separated from a certain

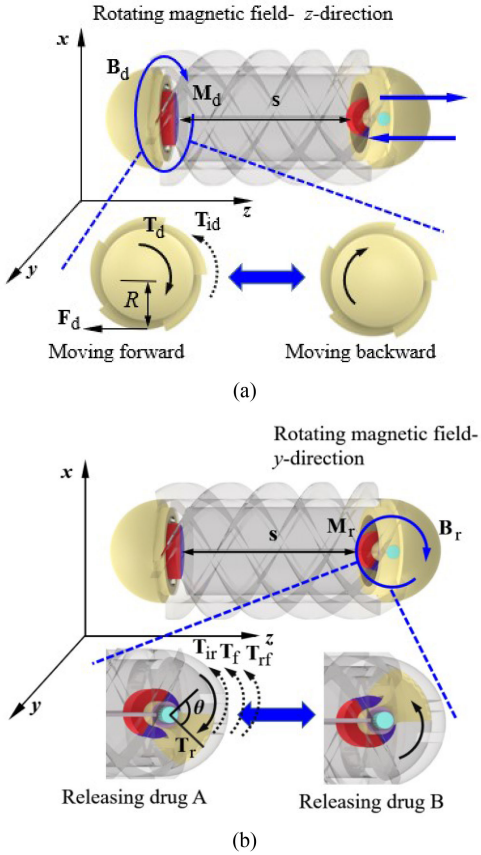

Fig. 5. Schematic diagram of motion analysis. (a) Locomotion. (b) Drug release.

distance [see Fig. 5(a)]. Therefore, the resultant torque of the driving magnet is

$$\boldsymbol{T}_{rd} = \boldsymbol{T}_d - \boldsymbol{T}_{id} \tag{1}$$

where $\boldsymbol{T}_d$ represents the torque exerted on the driving magnet by a rotating magnetic field and $\boldsymbol{T}_{id}$ indicates the torque of the driving magnet generated by the interaction between the driving magnet and the release magnet. Since the MCR moves in the intestine with spatial shape, these related parameters are all three-dimensional (3-D) vectors, e.g., $\boldsymbol{T}_{rd}, \boldsymbol{T}_d, \boldsymbol{T}_{id} \in \mathbb{R}^3$. A vector denoted as $\boldsymbol{T}_{rd}$ represents a three degree of freedom torque such that $\boldsymbol{T}_{rd} = [\boldsymbol{T}_{rdx}, \boldsymbol{T}_{rdy}, \boldsymbol{T}_{rdz}]^T$ with torques in three vertical directions. $\boldsymbol{T}_d$ is generated by the rotating magnetic field, and thus it is expressed as

$$\boldsymbol{T}_d = V_d \boldsymbol{M}_d \times \boldsymbol{B}_d \tag{2}$$

where V_d represents the volume of the driving magnet, $\boldsymbol{M}_d$ means the magnetization of the driving magnet, and $\boldsymbol{B}_d$ is the magnetic flux density of the rotating magnetic field applied to the driving magnet. The torque of the driving magnet generated by the interaction between the driving magnet and the release magnet is written as

$$\boldsymbol{T}_{id} = \frac{3\mu_0}{4\pi s^5} \boldsymbol{M}_d \times \boldsymbol{s} (\boldsymbol{M}_r \cdot \boldsymbol{s}) + \frac{\mu_0}{4\pi s^3} \boldsymbol{M}_r \times \boldsymbol{M}_d \tag{3}$$

where μ_0 is the permeability of the air and $\boldsymbol{s}$ represents the distance between the driving magnet and release magnet. The force on the edge of the spiral wing generated by the resultant torque of the driving magnet can be calculated by

$$\boldsymbol{T}_{rd} = \boldsymbol{F}_d \times \boldsymbol{R} \tag{4}$$

where $\boldsymbol{R}$ is the equivalent radius of the spiral wings interacting with the external environment. Based on these analyses and calculations, the viscosity and rotational speed of the robot can be obtained by combining with our previous calculations in [13].

As shown in Fig. 5(b), the rotating baffle changes the position relative to the grid plate to achieve the drug release and the rotation is affected by three types of resistances, which are generated by the driving magnet, the film, and rotation friction. The resultant torque of the release magnet can be expressed as

$$\boldsymbol{T}_{rr} = \boldsymbol{T}_r - \boldsymbol{T}_{ir} - \boldsymbol{T}_{rf} - \boldsymbol{T}_f \tag{5}$$

where $\boldsymbol{T}_r$ is the torque exerted on the release magnet by a rotating magnetic field, $\boldsymbol{T}_{ir}$ indicates the torque of the release magnet generated by the interaction between the driving magnet and the release magnet, $\boldsymbol{T}_{rf}$ is the resistance torque generated by the film during its motion with the rotating baffle, and $\boldsymbol{T}_f$ represents the friction torque generated during the rotation. The torque exerted on the release magnet by a rotating magnetic field is

$$\boldsymbol{T}_r = V_r \boldsymbol{M}_r \times \boldsymbol{B}_r \tag{6}$$

where V_r is the volume of the release magnet, $\boldsymbol{M}_r$ indicates the magnetization of the release magnet, and $\boldsymbol{B}_r$ is the magnetic flux density of the rotating magnetic field applied to the release magnet. The torque of the release magnet generated by the interaction between the driving magnet and the release magnet is written as

$$\boldsymbol{T}_{ir} = \frac{3\mu_0}{4\pi s^5} \boldsymbol{M}_r \times \boldsymbol{s} (\boldsymbol{M}_d \cdot \boldsymbol{s}) + \frac{\mu_0}{4\pi s^3} \boldsymbol{M}_d \times \boldsymbol{M}_r. \tag{7}$$

During the process of drug release, the rotating baffle starts to rotate from a static status with the rotation of the rotating magnetic field, and it will have the same rotational speed as the rotating magnetic field after acceleration. Then the rotating baffle rotates to the required positions with the rotating magnetic field. The parameters during the acceleration can be calculated by

$$\begin{bmatrix} \boldsymbol{\alpha} \\ \boldsymbol{\omega} \cdot \boldsymbol{\omega} \end{bmatrix} = \begin{bmatrix} \frac{1}{J} \boldsymbol{T}_{rr} \\ 2\boldsymbol{\theta} \cdot \boldsymbol{\alpha} \end{bmatrix} \tag{8}$$

where $\boldsymbol{\alpha}$ is the angular acceleration of the rotating baffle, J is the equivalent moment of inertia of the rotating baffle (including the release magnet, shaft, etc.), $\boldsymbol{\omega}$ is the angular velocity of the rotating baffle, and $\boldsymbol{\theta}$ is the rotation angle of the rotating baffle. The MCR has spatial motion parameters as it advances in the intestine and these motion parameters can be obtained by the above equations with vectors belon ging to $\mathbb{R}^3$.

D. Dual-Drug Release Control

Due to the complex environment in the intestine, it is difficult to achieve precision control of the movement of the capsule

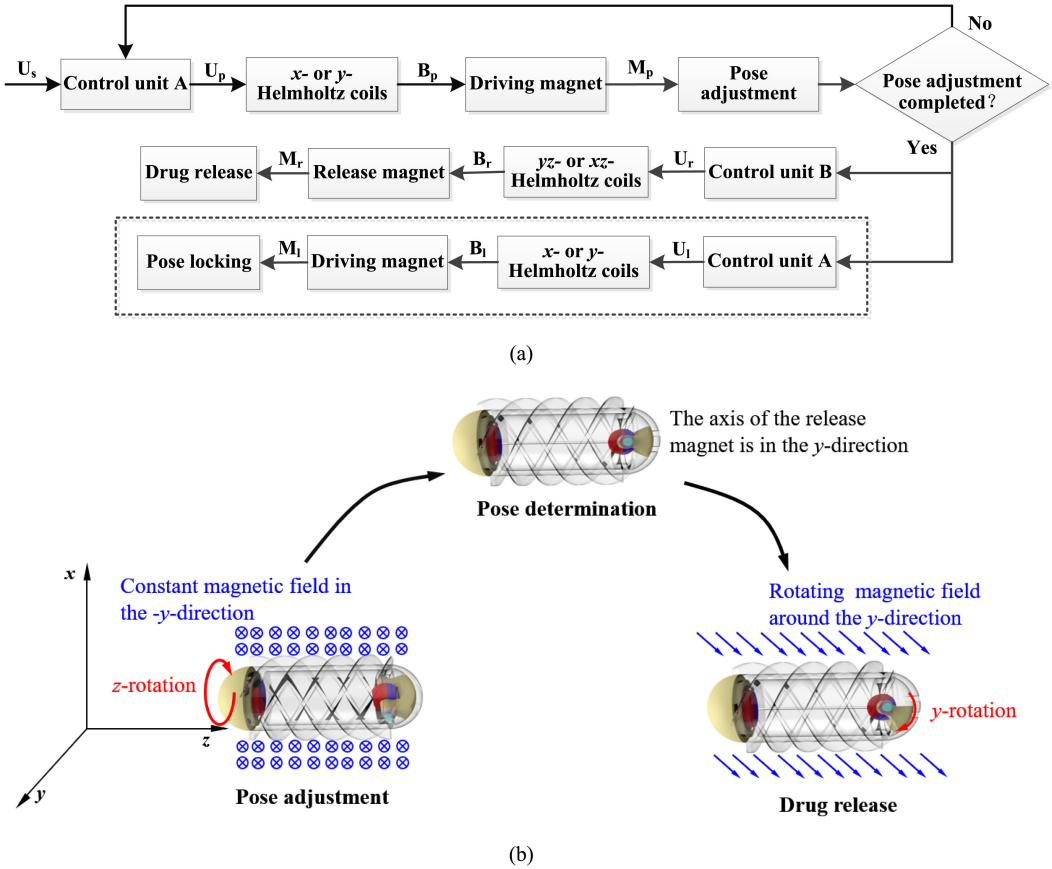

Fig. 6. Drug release control. (a) Flowchart of the control method for the drug release. (b) Process diagram of the drug release control. U_s is the control voltage sent from the control panel when surgeons operate, U_p is the driving voltage of the Helmholtz coils, B_p is the magnetic flux density of the constant magnetic field, and M_p is the torque applied to the MCR; U_r is the control voltage used for drug release, B_r is the magnetic flux density of the rotating magnetic field, and M_r is the torque for drug release; and U_l is the control voltage used for pose locking, B_l is the magnetic flux density of the constant magnetic field for pose locking, and M_l is the torque for pose locking.

robot. Some common methods, for example, the closed-loop control, need additional instruments/sensors to obtain feedback signals, thus increasing the manufacturing difficulty and cost and decreasing the RDC of capsule robots. Therefore, there are three considerations for the drug release control: no modifications to existing equipment; no additional components; and using open-loop control to achieve the dual-drug release. In this article, based on the proposed drug release mechanism, a control method for the MCR is presented to achieve dual-drug release. This method uses one-directional Helmholtz coils, e.g., *x*-Helmholtz coils, to adjust the pose of the MCR, and adopts the other two Helmholtz coils, e.g., *y*- and *z*-Helmholtz coils, to control the drug release mechanism. The flowchart of the control method is shown in Fig. 6(a).

The *x*- or *y*-Helmholtz coils generate a constant magnetic field when surgeons operate the control panel and the MCR start to adjust its pose with the torque M_p produced by the driving magnet in the constant magnetic field. After this procedure, completion of the pose adjustment should be determined for the next operation. The judgment method we adopt is to repeat the above process and use the orientation of the magnetic field to ensure the completion of pose adjustment. The judgment condition is time-that is, the pose adjustment is considered completed after a period of time, e.g., 0.5 s. Then, the control unit drives *yz*- or *xz*-Helmholtz coils to produce a rotating magnetic field that controls the release magnet. The rotary direction of the rotating magnetic field determines the type of released drugs. The drug release mechanism was designed to have two limit positions for selective release. As shown in Fig. 4(c), the release magnet rotates forward and it will be stopped at the lower limit position; the release magnet rotates in reverse and then is halted at the upper limit position [see Fig. 4(e)]. During this procedure, the release magnet keeps driving the rotating baffle to rotate without any feedback, and different drugs are released when the rotating baffle reaches various limit positions. There is no need to accurately control the release magnet's rotation angle, which reduces the difficulty of control and improves the control reliability and adaptability to complex environments. Moreover, to improve the stability of pose maintenance during drug release, a constant magnetic field can also be produced to lock the MCR pose and this operation is similar to the pose adjustment [shown in the dashed box of Fig. 6(a)]. During drug release, the rotating magnetic field and constant magnetic field are produced by different Helmholtz coils and there will be no conflict of usage requirements for Helmholtz coils. Therefore, this method realizes stable control of dual-drug release with the

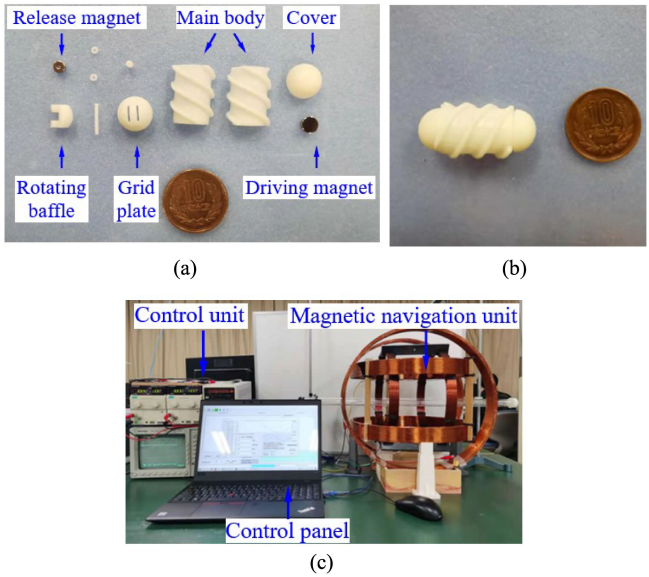

Fig. 7. Proposed robot system. (a) Manufactured components. (b) Assembled MCR. (c) System overview.

TABLE I
SPECIFICATIONS OF THE MAGNETIC NAVIGATION UNIT

Direction	Diameter (mm)	Coil turns	Wire diameter (mm)	Material	Resistance (Ω)
x	284	125	1.5	Cu	2.4
y	350	150	1.5	Cu	3.3
z	400	180	1.5	Cu	4.5

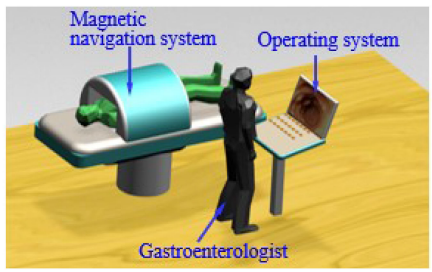

Fig. 8. Diagram of the upgraded robot system.

open-loop control and without changing the existing equipment and adding additional components.

Fig. 6(b) shows an example of this control process. In the beginning, the MCR pose is random, i.e., the direction of the release magnet axis relative to the magnetic field is unknown. In the pose adjustment, a constant magnetic field in the -y-direction is generated by y-Helmholtz coils and the MCR will rotate around the z-direction. The MCR pose is then determined and the axis of the release magnet is in the y-direction. Then, during the dual-drug release, x- and z-Helmholtz coils produce a rotating magnetic field around the y-direction and the release magnet rotates around the y- and y-directions to release various drugs.

E. Prototype and Robot System

The proposed MCR was fabricated by 3-D printing and assembled manually in the laboratory. The prototype is shown in Fig. 7(a) and (b). A cylindrical magnet (NO260, NeoMag, JP) is used as the driving magnet while the other magnet (NOR047, NeoMag, JP) works as the release magnet. The assembled robot has the dimensions of Φ14 mm $\times$ 28.9 mm and and an RDC of 0.46 and weighs 3.47 g. The dimensions could be further optimized based on clinical requirements and the types of magnets would be changed accordingly. The generated torques for the driving magnet or release magnet can be adjusted by changing the magnetic flux density of the rotating magnetic field and thus the required torques for robot motion or drug release will be obtained when the magnetization of the driving magnet changes with the replacement of different types of magnets. Fig. 7(c) shows the overview of the robot system. A magnetic navigation unit, consisting of x-directional Helmholtz coils, y-directional Helmholtz coils, and z-directional Helmholtz coils, is used to generate magnetic fields. Specifications of the magnetic navigation unit are given in Table I. Operators input the control information through the control panel and the control information is then transferred to the voltage signals through the control unit. With these voltage signals, the magnetic navigation unit generates specific rotating magnetic fields when it is powered by the power unit and then the required motion of the robot will be achieved.

F. Clinical Considerations

In future clinical applications, the proposed robot system needs to be upgraded and integrated with the clinical environment. The possible diagram of the upgraded robot system is shown in Fig. 8. The upgraded robot system is composed of a magnetic navigation system and operating system. The magnetic navigation system comprises three sets of Helmholtz coils similar to the magnetic navigation unit in Fig. 7(c), but can produce magnetic fields with greater intensities. Gastroenterologists manipulate capsule robots through the operating system. The proposed MCR will also be able to capture the intestinal image when a camera is assembled in the cover (see Fig. 2). In the treatment procedures, patients swallow the MCR and then lie down in the magnetic navigation system on an operating table. The MCR can be remotely controlled by gastroenterologists through the operating system.

The surface of the MCR is not that smooth due to the spiral wings set on it. These spiral wings may rub against the surface of the tissue and cause damages. The gaps between spiral wings can be filled with edible and soluble materials, such as ice, gelatin, and soluble sugar. Thus the surface of the MCR would be much smoother and is easy to swallow without damage to the tissue, and the spiral wing can return to the original shape and generate the driving force with rotation when the MCR enters the intestine and the filled materials have melted. Moreover, the spiral wing can also be made of edible and soluble materials with a long melting time and this will eliminate the tissue injuries when the MCR is discharged from the anus after it melts.

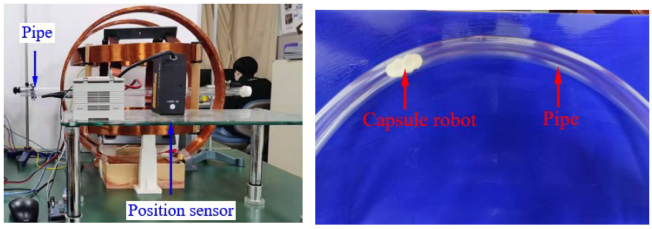

(a) (b)

Fig. 9. Locomotion experiments. (a) Experimental setup. (b) Bent pipes placed on a board.

III. Performance Evaluation

A. Locomotion

1) Experimental Setup: The MCR moves to the target position first with the rotating magnetic field and then starts to release drugs. Various magnetic frequencies result in different moving velocities of the MCR. Besides, after releasing drugs, the weight of the robot will be reduced. MCRs with different weights will have various moving velocities. Thus, to test the moving velocities of the MCR with various magnetic frequencies and weights, experiments were carried out and the experimental setup is shown in Fig. 9 (named as experiment I). The MCR was located in a pipe with an internal diameter of 18 mm. The pipe was placed in the Helmholtz coils that generate magnetic fields to drive the MCR. A laser displacement sensor (LK-500, KEYENCE, JP) was used to assist the moving velocity measurement. Start and stop lines were marked in the pipe and the MCR moved from the start line to the stop line. The laser displacement sensor was positioned near the stop line and can output readings when the MCR moved to the stop line. The Helmholtz coils and the laser displacement sensor were turned on simultaneously. When the MCR moved to the stop line, i.e., moving forward, the readings of the laser displacement sensor changed and the moving time was then obtained based on this. The moving velocities of the MCR were calculated through the moving displacement and time. Similarly, the MCR moved from the stop line to the start line, i.e., moving backward, and the moving velocities were also calculated. The magnetic frequency for every single movement was set as 1 HZ with 1-HZ increment over a range of 8Hz, and each moving velocity of the MCR with the corresponding magnetic frequency was calculated. Besides, the MCR loading drugs of various weights was used for these measurements. The drug weights were set as 0, 0.5, 1, and 1.5 g since the MCR is able to load up to 1.5 g of drugs. Every measurement was repeated ten times and the standard deviations were calculated.

Additionally, to evaluate the movement performance of the MCR in the bent route, similar experiments were carried out in pipes with various radii of curvature (named as experiment II). Pipes with different radii of curvature were fabricated and placed on a board. As shown in Fig. 9(b), the bent pipe has the same internal diameter as that in experiment I and was placed in the Helmholtz coils during the experiments. The radii of curvature of the pipes were set as 225, 175, 125, 75, and 25 mm. The magnetic frequency was set as 4 Hz. The experimental procedures, data acquisition, and processing methods were the same as those in Experiment I.

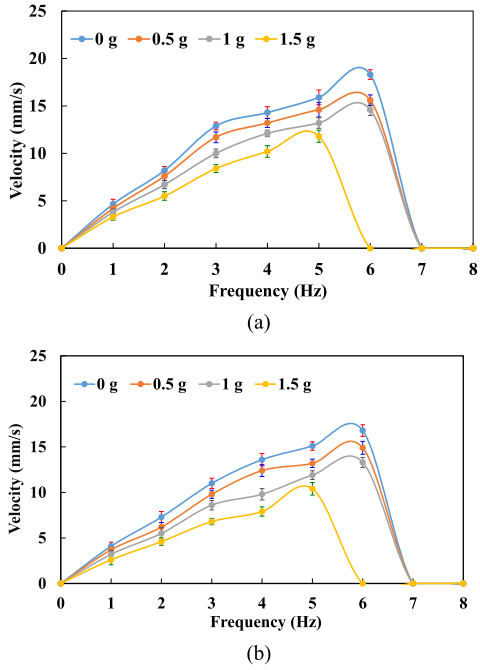

Fig. 10. Moving velocities of the MCR with various loads and magnetic frequencies. (a) MCR moving forward. (b) MCR moving backward.

2) Results and Discussion

The moving velocities of the MCR loading drugs of various weights and driven by magnetic fields with different frequencies were calculated and shown in Fig. 10. The maximum advance velocities of the MCR loading drugs of 0, 0.5, 1, and 1.5 g, are 18.3, 15.6, 14.6, and 11.8 mm/s, respectively. The maximum retreat velocities of the MCR loading drugs of 0, 0.5, 1, and 1.5 g, are 16.8, 14.9, 13.3, and 10.4 mm/s, respectively. The curve trend indicates that the MCR has great velocities when magnetic fields with larger frequencies are applied. This is mainly because magnetic fields with larger frequencies produce great rotary velocities that result in more significant moving velocities. However, this trend of velocity increase with magnetic frequency growth is effective in a certain range. As we discussed in the previous research [13], every MCR has a step-out frequency and it cannot start to rotate when the magnetic frequency is larger than this frequency. As shown in Fig. 10, the velocity of the MCR with a drug of 1.5 g is 0 when the magnetic frequency is 6 Hz since the step-out frequency of the MCR with a load of 1.5 g drug is less than 6 Hz. Besides, advance velocities have great values than retreat velocities because the shape of the cover differs from that of the drug release mechanism [see Figs. 2 and Fig. 4], and they will produce various resistance when the MCR moves forward and backward.

Fig. 10 shows that heavier drugs reduce the moving velocities of the MCR. For example, the advance velocities of the MCR loading drugs of 0, 0.5, 1, and 1.5 g, are 14.3, 13.2, 12.1, and 10.2 mm/s, respectively, when the magnetic frequency is 4 Hz. This

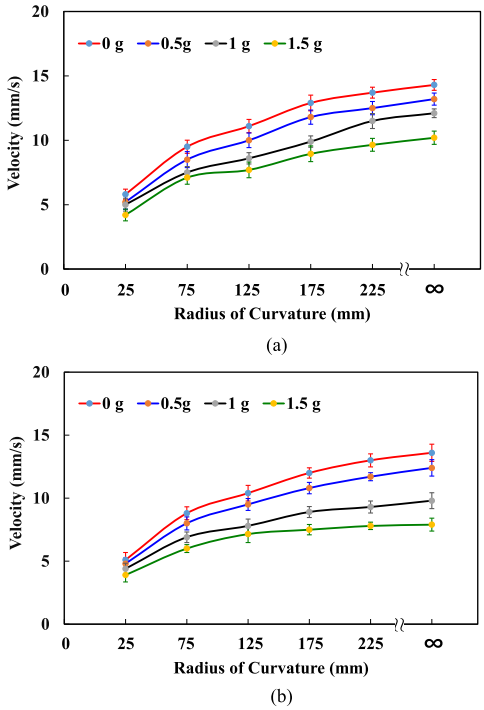

Fig. 11. Moving velocities of the MCR driven by a magnetic field of 4 Hz in pipes with various radii of curvature. (a) MCR moving forward. (b) MCR moving backward.

tendency is mainly due to the fact that 1) great weight brings in bigger frictions with the pipe that hinders the movement of the MCR, and 2) great weight will increase the moment of inertia of the MCR, which is not conducive to the rotation. Although the weight of loaded drugs affects the moving velocity of the MCR, this impact is not that serious. Moreover, there will be a special positioning system to assist robots in moving to the target position during drug releases, such as camera-based positioning or external magnetic field positioning. The robots do not rely on the moving velocity control to complete drug releases, and thus, the moving velocity that changes with the weight of drugs will not affect the drug release.

In experiment II, the velocities of the MCR with various loads in different pipes were calculated and shown in Fig. 11. In addition, since the straight pipe used in experiment I can be considered a pipe with an infinite radius of curvature, the data from Experiment I were added to Fig. 11. With the comparison of Fig. 11(a) and (b), we found the advance velocity has a larger value than the retreat velocity in all trials. These advance and retreat situations are similar to experiment I. The drug release mechanism of the MCR will always produce greater resistance to movement than the cover of the MCR in various working conditions and environments.

Besides, the velocity of the MCR drops as the radius of curvature of the pipe decreases. We think this is caused by the following two reasons.

1) The axis of the curved pipe does not coincide with the moving direction of the MCR and they form an included angle. The resistance of the pipe to the MCR raises with the increase of the included angle. The pipe has little resistance to the MCR when the included angle is 0°; the MCR cannot advance as the included angle equals 90°.
2) The MCR will keep turning when it moves in the bent pipe and this continuous steering requires additional kinetic energy, thus resulting in lower moving velocity. [19] shows that the minimum radius of curvature of the intestine for humans is about 25 mm. In these experiments, the minimum radius of curvature of the pipes is set to 25 mm, and thus, basically, this setup could be acceptable.

These experimental results demonstrated the ability of the MCR to move in the bent pipes that provides the possibility to release drugs in various intestine areas.

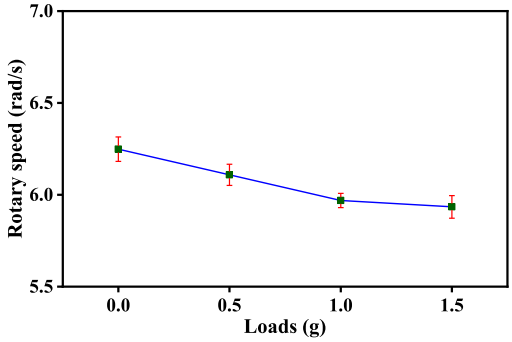

Fig. 12. Rotary speeds of the rotating baffle with various drug loadings.

B. Drug Release Control

1) Experimental Setup: In order to test the drug release performance of the MCR, drug release control experiments were conducted. The experimental setup is similar to that in Section III-A. A pipe with the MCR is positioned in the Helmholtz coils. The Helmholtz coils produce magnetic fields to the drug release mechanism of the MCR. The drug release mechanism has two limit positions and the rotating baffle can move between them [see Fig. 4(b) and (e)]. In this article, the angle formed by these two extreme positions is 76°. The rotating baffle was positioned at one position and rotated to the other position with the magnetic fields. To verify the effect of the drug weight on the rotation of the rotating baffle, the rotating baffle rotated with different weights of drugs. Since the maximum drug loading capacity of the MCR is 1.5 g, the weight of the loaded drug for each experiment was set as 0, 0.5, 1, and 1.5 g. The magnetic frequency was set as 1 Hz. The rotary time was recorded and then the rotary speed was calculated. Every measurement was repeated ten times and the standard deviations were calculated.

2) Results and Discussion: Fig. 12 shows the rotary speeds of the rotating baffle with various drug loadings. The maximum and minimum rotary speeds of the rotating baffle are 6.25 and 5.93 rad/s, respectively. The lower rotary speed of the rotating baffle occurred as the MCR loaded heavier drugs; the higher rotary speed of the rotating baffle arose when the lighter drug was carried. Drug weight affects the rotary speed of the rotating baffle. The loaded drug exerts pressure on the rotating baffle, and this pressure impedes the rotation of the rotating baffle. So

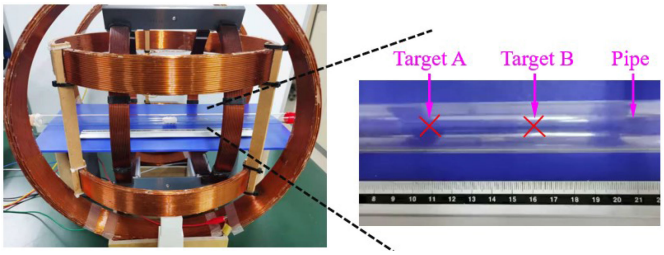

Fig. 13. Experimental setup for dual-drug release test.

great drug weight results in lower rotary speed. When the MCR is fully loaded (i.e., loading 1.5 g drug), the rotary speed is the lowest, 5.93 rad/s. This rotary speed can ensure the MCR opens the rotating baffle (grid plate) for drug release in 1.06 s, and this speed would be acceptable for drug release.

C. Dual-Drug Release

1) Experimental Setup: To verify whether the MCR can complete the dual-drug release, experiments were designed to test the performance of the MCR moving to various target positions to release different drugs. The experimental setup is the same as that in the previous experiments. A pipe marked targets A and B was used and located in the Helmholtz coils (see Fig. 13). Two types of water, dyed red and black, used to replace drugs A and B, were injected into compartment A and compartment B of the MCR, respectively. Helmholtz coils were used to produce magnetic fields with various directions to realize different functions of the MCR. A rotating magnetic field with z-direction [see Fig. 5(a)] was generated first to rotate the main body of the MCR and then the MCR moved forward. When the MCR moved to target A, it stopped and a constant magnetic field in the y-direction was then generated. The rotating baffle started to rotate in the clockwise direction when x- and z-Helmholtz coils produced a rotating magnetic field around the y-direction. The red water (drug A) was released at target A. Similarly, the MCR moved to target B and released the black water (drug B). All entire movements were videotaped by a camera.

2) Results and Discussion: The MCR tried to release two types of drugs at targets A and B ten times, and it all completed this task successfully. The video snapshots of the movement procedure are shown in Fig. 14. The MCR released drug A at target A and released drug B at target B. In Fig. 14(c), (d), and (f), the released drugs A and B are not just located at targets A and B, but spread to other places. This is because the water has fluidity and can flow with the movement of the MCR. Before the MCR releases the drugs, the release magnet of the drug release mechanism needs to be adjusted in a suitable position relative to the magnetic field, which will enable the rotating baffle to rotate in the expected direction. In these experiments, the pose of the MCR was adjusted by the proposed drug release control method that eliminates the detection and accurate control of the pose. On the other hand, the operator easily obtained the MCR position relative to the targets and stopped the MCR near the targets since the pipe is transparent. In practical applications, the operator can

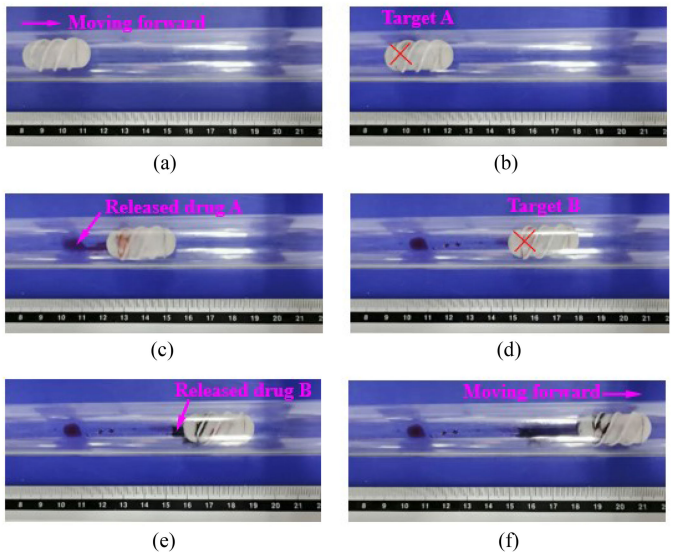

Fig. 14. Dual-drug release procedure. (a) MCR moved toward target A. (b) MCR stopped at target A and started to release drug A. (c) Drug A was released and the MCR started to move toward target B. (d) MCR moved to target B and stopped. (e) MCR released drug B. (f) MCR kept moving forward.

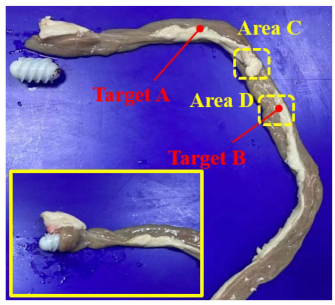

Fig. 15. Experimental setup for *ex vivo* experiments. Targets A and B were drug release points and areas C and D were used as observation areas of intestinal damage.

not directly obtain the position of the MCR relative to targets, so assisted devices are needed for navigation, such as magnetic field positioning devices and cameras. In addition, the MCR will have more potential applications when it is integrated with other technologies, including complex position and velocity control [20], [21], and visual perception [22].

D. Ex Vivo Experiments

1) Experimental Setup: To test the possibility of clinical application of the MCR, *ex vivo* experiments were carried out. A pig intestine was used to simulate the human intestine. The pig intestine was acquired from a food supplier and there is no ethics required. As shown in Fig. 15, the intestine was placed on a plate and the MCR could be put into the intestine from the incision. Two targets were marked in the intestine and the MCR was set to release two different drugs near these two targets. Red and blue water were loaded into the MCR to replace drugs. The experimental procedures were the same as the experiments in Section III-C. Moreover, to evaluate the damage of the MCR

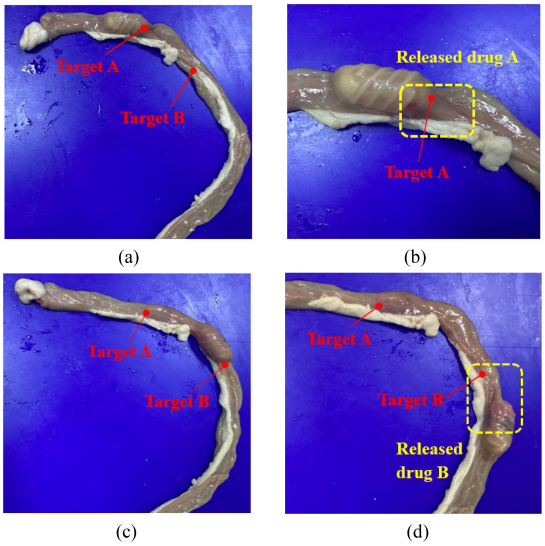

Fig. 16. Locomotion and drug release process. (a) MCR moved to target A from the incision of the intestine and prepared to release drug A. (b) Drug A was released. (c) MCR moved to target B and released drug B. (d) MCR continued to move forward.

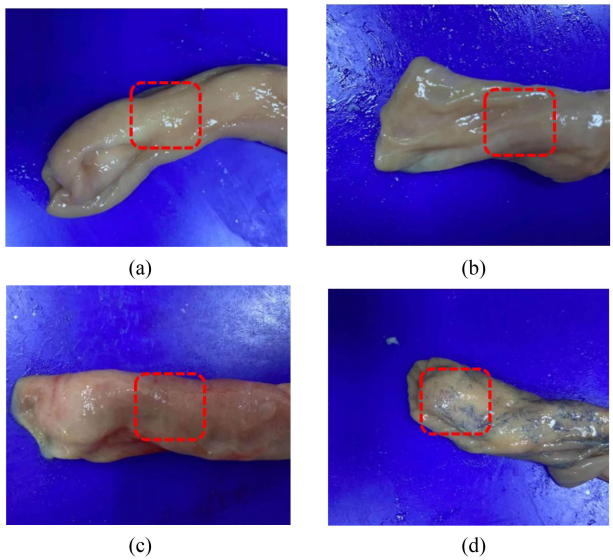

Fig. 17. Observation areas photographed before and after experiments. (a) and (b). Areas C and D before experiments. (c) and (d) Areas C and D after experiments.

to the intestinal wall, photos of the internal wall were taken for comparison before and after the operation. Two areas of the intestinal wall, located on movement path and drug release position, i.e., areas C and D, were selected for observation.

2) Results and Discussion: The MCR completed these two tasks and the process is shown in Fig. 16. The MCR started to move towards target A under the rotating magnetic field for locomotion (4 Hz). It stopped at target A when the rotating magnetic field for locomotion was shut down [see Fig. 16(a)]. After the pose adjustment with a constant magnetic field, the rotating magnetic field for drug delivery started to work at 1 Hz and drug A was then released. As shown in the yellow dashed box in Fig. 16(b), part of the instestinal wall was dyed red. After the release, the rotating magnetic field for locomotion began to work at 3 Hz and the MCR reached target B. As shown in Fig. 16(c) and (d), the MCR released drug B and then moved forward. Released drug B can be seen on the spiral wings of the MCR that are dyed blue. In this experiment, drugs A and B were successfully delivered at targets A and B, respectively. These experiments show the possible ability of the proposed MCR to perform various tasks in complex environments. The experimental settings might not fully simulate the actual human intestine and might not characterize the usability of the MCR strictly, but they can be regarded as a good first approximation.

The lining of the intestine was turned out and photographed before and after experiments. The photos of the selected areas are shown in Fig. 17. Fig. 17(c) and (d) have a darker intestinal wall than Fig. 17(a) and (b) since the wall was dyed with the released drugs. With the comparison of these photos, no noticeable difference was observed to the naked eyes. This "no noticeable difference" could not strictly demonstrate the MCR produces no injuries to the intestine. Specific injury assessment requires professional medical assessment, especially microscopes. The professional medical assessment was not performed currently, but this elementary assessment using naked eye observation can preliminarily show the injury level of the MCR to the intestine. The worst situation for this "no noticeable difference" is a slight injury to the intestinal wall. Since this kind of injury is not visible to the naked eyes, this possible slight injury would not seriously affect the patients' rehabilitation or operation safety. In addition, in these experiments, the MCR was fabricated through 3-D printing and the spiral wings on the surface of the MCR have a high hardness that might scratch the intestinal wall. In future applications, soft materials will be employed to fabricate the spiral wings, which can not only further reduce the injuries to the intestine but also facilitate the swallowing of patients.

Besides, some current capsule robots were selected and their characteristics were given in Table II for comparison. These capsule robots are powered by two different methods to achieve locomotion and drug delivery, resulting in different advantages and disadvantages. In contrast with batteries, magnetic fields have higher safety for patients since batteries may bring potential danger when they are in the intestine [17]. For example, in [11], the battery activates the coils to generate huge magnetic fields that can push and open the drug release cage. During this procedure, a massive current is required and this would introduce safety issues. Besides, the drug may be demanded to be released in various positions during the treatment, which brings a requirement on the multiple release control of one drug. Many current capsule robots possess this multiple release control and can release the drug multiple times when various positions need the drug, except for the robot in [23], even though it has good performance in incorporating both the anchoring and release mechanism. Munoz *et al.* [10] indicates the importance of high RDC as well as the minimum RDC value for the capsule robots, and Beccani *et al.* [11] and the proposed MCR have achieved this goal (i.e., RDC$\geq$0.4), which means relatively sufficient drugs

TABLE II
SELECTED CHARACTERISTIC COMPARISON OF CAPSULE ROBOTS

Group	Powered by	Number of drugs released	RDC	Multiple releases	Dimensions
[7]	Magnetic field	One	0.16	Yes	Φ13.5mm×31mm
[8]	Battery	One	0.28	Yes	Φ11mm×30 mm
[11]	Battery	One	0.6	Yes	Φ13mm×30 mm
[23]	Magnetic field	One	0.07	No	Φ15mm×40 mm
Proposed MCR	Magnetic field	Two	0.46	Yes	Φ14 mm×28.9 mm

RDC: ratio of the volume of loaded drug to the total volume of the capsule.

can be loaded to ensure the effectiveness of treatment. Additionally, our proposed MCR also addresses the other limitation mentioned in Section I, i.e., multidrug delivery. As given in Table II, the MCR has similar dimensions to existing research, but it still seems bigger than the required swallowable volume (i.e., $\Phi 11$ mm $\times$ 26 mm [9]). The dimensions of the MCR are mainly affected by the Helmholtz coils. The Helmholtz coils used in this article cannot generate a great-intensity magnetic field due to their limited size and physical characteristics. Thus, based on (2) and (6), we used permanent magnets with significant volumes, resulting in the developed MCR with large dimensions. Since great Helmholtz coils will be adopted in the further application, the MCR will have small dimensions. These reduced dimensions will allow the MCR to be much more swallowable and to pass through pipes with smaller radii of curvature.

IV. CONCLUSION

In this article, a dual-drug delivery concept was presented, and based on this concept, a capsule robot with selective dual-drug delivery and a control method were proposed. The developed robot has a high RDC and can move in the intestine and release two different drugs at various target positions. These proposed methods allow one active capsule robot to perform more complex treatments, eliminate the use of multiple robots to complete various drugs release, have a high RDC to load a sufficient dosage for treatment, and have a low cost and simple structure without modification of existing equipment. The performance was evaluated through *in vitro* and *ex vivo* experiments and the experiment results show good performance of this proposed MCR. Moreover, this proposed MCR has good expansibility and would have potential further applications when integrated with the module capsule robots presented in our previous research [13]. Optimizations of the dimensions, swallowability, and discharge of the proposed MCR need to be carried out to meet the clinical requirements comprehensively. In our future work, we will complete these optimizations and test the performance through animal experiments.

REFERENCES

[1] L. W. Day, D. Siao, J. M. Inadomi, and M. Somsouk, "Non-physician performane of lower and upper endoscopy: A systematic review and meta-analysis," *Endoscopy*, vol. 46, no. 5, pp. 401–410, 2014.
[2] G. Ciuti *et al.*, "Frontiers of robotic endoscopic capsules: A review," *J. Micro-Bio Robot.*, vol. 11, no. 1, pp. 1–18, May 2016.
[3] G. Iddan, G. Meron, A. Glukhovsky, and P. Swain, "Wireless capsule endoscopy," *Nature*, vol. 405, pp. 417–418, 2000.
[4] M. Sitti *et al.*, "Biomedical applications of untethered mobile milli/microrobots," *Proc. IEEE*, vol. 103, no. 2, pp. 205–224, Feb. 2015.
[5] R. W. J. Westerhof and J. Koornstra, "Risk factors for incomplete small-bowel capsule endoscopy," *Gastrointestinal Endoscopy*, vol. 69, pp. 74–80, 2009.
[6] J. Nam, W. Lee, J. Kim, and G. Jang, "Magnetic helical robot for targeted drug-delivery in tubular environments," *IEEE/ASME Trans. Mechatronics*, vol. 22, no. 6, pp. 2461–2468, Dec. 2017.
[7] S. H. Kim and K. Ishiyama, "Magnetic robot and manipulation for active-locomotion with targeted drug release," *IEEE/ASME Trans. Mechatronics*, vol. 19, no. 5, pp. 1651–1659, Oct. 2014.
[8] X. Guo, Z. Luo, H. Cui, and Q. Jiang, "A novel and reproducible release mechanism for a drug-delivery system in the gastrointestinal tract," *Biomed. Microdevices,* vol. 21, no. 1, 2019, Art. no. 25.
[9] P. Valdastri, R. J. Webster, C. Quaglia, M. Quirini, A. Menciassi, and P. Dario, "A new mechanism for mesoscale legged locomotion in compliant tubular environments," *IEEE Trans. Robot.*, vol. 25, no. 5, pp. 1047–1057, Oct. 2009.
[10] F. Munoz, G. Alici, and W. Li, "A review of drug delivery systems for capsule endoscopy," *Adv. Drug Del. Rev.*, vol. 71, pp. 77–85, May 2014.
[11] M. Beccani, C. D. Natali, G. Aiello, C. Benjamin, E. Susilo, and P. Valdastri, "A magnetic drug delivery capsule based on a coil actuation mechanism," *Procedia Eng.,* vol. 120, pp. 53–56, 2015.
[12] L. Zheng, S. Guo, and Z. Wang, "Performance evaluation of an outer spiral microrobot in pipes in different environments," in *Proc. IEEE Int. Conf. Mechatronics Automat.*, Oct. 2020, pp. 643–647.
[13] L. Zheng, S. Guo, Z. Wang, and T. Tamiya, "A multi-functional module-based capsule robot," *IEEE Sens. J.*, vol. 21, no. 10, pp. 12057–12067, May 2021.
[14] Z. Wang, S. Guo, J. Guo, Q. Fu, L. Zheng, and T. Tamiya, "Selective motion control of a novel magnetic driven minirobot with targeted drug sustained-release function," *IEEE/ASME Trans. Mechatronics*, to be published, doi: 10.1109/TMECH.2021.3063750.
[15] Z. Wang, S. Guo, Q. Fu, and J. Guo, "Characteristic evaluation of a magnetic-actuated microrobot in pipe with screw jet motion," *Microsyst. Technol.*, vol. 25, no. 6, pp. 719–727, 2019.
[16] Q. Fu, S. Zhang, S. Guo, and J. Guo, "Performance evaluation of a magnetically actuated capsule microrobotic system for medical applications," *Micromachines*, vol. 9, no. 12, pp. 641–657, 2018.
[17] G. Ciuti, A. Menciassi, and P. Dario, "Capsule endoscopy: From current achievements to open challenges," *IEEE Rev. Biomed. Eng.*, vol. 4, pp. 59–72, Oct. 2011.
[18] L. Liu, S. Towfighian, and A. Hila, "A review of locomotion systems for capsule endoscopy," *IEEE Rev. Biomed. Eng.*, vol. 8, pp. 138–151, Jun. 2015.
[19] J. Choi, "Design and development of a minimally invasive endoscope: Highly flexible stem with large deflection and stiffenable exoskeleton structure," Ph.D. dissertation, Dept. Mech. Eng., Virginia Tech., Blacksburg, VA, USA, 2006.
[20] M. Fruchard, L. Sadelli, and A. Ferreira, "Local controllability, trajectory planning, and stabilization of a two-agent underactuated microrobotic system," *IEEE Syst. J.*, vol. 14, no. 2, pp. 2892–2900, Jun. 2020.
[21] J. T. Shepard and C. A. Kitts, "A multirobot control architecture for collaborative missions comprised of tightly coupled, interconnected tasks," *IEEE Syst. J.*, vol. 12, no. 2, pp. 1435–1446, Jun. 2018.
[22] E. Benli, Y. Motai, and J. Rogers, "Visual perception for multiple human-robot interaction from motion behavior," *IEEE Syst. J.*, vol. 14, no. 2, pp. 2937–2948, Jun. 2020.
[23] S. Yim and M. Sitti, "Design and rolling locomotion of a magnetically actuated soft capsule endoscope," *IEEE Trans. Robot.*, vol. 28, no. 1, pp. 183–194, Feb. 2012.

Lingling Zheng (Student Member, IEEE) received the M.S. degree in electrical and information engineering from the Anhui University of Technology, Anhui, China, in 2018. She is currently working toward the Ph.D. degree in intelligent mechanical systems engineering with the Faculty of Engineering and Design, Kagawa University, Takamatsu, Japan.

Her research interests include microrobot and medical robots, especially capsule robot systems.

Shuxiang Guo (Fellow, IEEE) received the Ph.D. degree in mechano-informatics and systems from Nagoya University, Aichi, Japan, in 1995.

He is currently a Full Professor with the Department of Intelligent Mechanical Systems Engineering, Faculty of Engineering and Design, Kagawa University, Takamatsu, Japan. He is currently the Chair Professor with the Key Laboratory of Convergence Medical Engineering System and Healthcare Technology, Ministry of Industry and Information Technology, Beijing Institute of Technology, Beijing, China. His research interests include medical robot systems, microcatheter systems, and biomimetic underwater robots.

Dr. Guo is currently the Editor-in-Chief of the *International Journal of Mechatronics and Automation*.

Masahiko Kawanishi received the B.S. degree in medicine from the Faculty of Medicine of Kagawa Medical University, Kagawa, Japan, in 1993.

He is currently an Associate Professor with the Faculty of Medicine, Kagawa University, Takamatsu, Japan. He has authored or coauthored more than 80 refereed journal and conference papers.

His research interests include the surgical techniques of neurosurgical operations and intravascular surgery system.